Thermal stability of oxygen vacancy stabilized zirconia (OVSZ) thin films

Mohsin Raza[*,a], Pascal Boulet[b], Jean-François Pierson[b], Rony Snyders[a,c] and Stephanos Konstantinidis[a]

[a] Chimie des Interactions Plasma-Surface (ChIPS), University of Mons, 23 Place du Parc, 7000 Mons, Belgium.

E-mail: mohsinraza.khan@outlook.com; stephanos.konstantinidis@umons.ac.be

[b] Institut Jean Lamour (UMR CNRS 7198), Université de Lorraine, Campus ARTEM, 54011 Nancy Cedex, France

[c] Materia Nova Research Center, Parc Initialis, B-7000 Mons, Belgium

Keywords: Cubic zirconia, Phase transformation, Thermal stability, Oxygen vacancy, Stress

Abstract:

Thermal stability of oxygen vacancy stabilized cubic zirconia (OVSZ) thin films containing 16 and 3 at.% oxygen vacancies, synthesized by reactive magnetron sputter deposition, is reported. Temperature-resolved grazing incidence X-ray diffraction (TR-GIXRD) measurements (200-900 °C) in air and nitrogen ambient were performed. TR-GIXRD data show the deposited films are stable up to 750 °C irrespective of the annealing ambient or the oxygen vacancy concentration. However, above 750 °C a fraction of zirconia cubic crystals transforms into monoclinic crystals. Transformation of a fraction of zirconia cubic crystals into monoclinic crystals is explained by taking into account the compressive stresses generated as a result of

[*]Corresponding author, currently working at Thin Film Physics group, Department of Physics, Chemistry and Biology (IFM), Linköping University, Sweden.

discrepancy in film-substrate thermal expansion coefficients. Thermal cycling of the deposited OVSZ thin films is also performed at 700 °C and show films retain their pure *c*-phase.

Introduction

In order for materials to work properly, particularly in the case of materials for high temperature applications, materials have to be stable chemically and structurally at elevated temperatures as the materials properties are very much dependent on these two factors [1,2]. One example of this is zirconia (ZrO_2), a material of high importance for many high temperature applications. Zirconia is a polymorphic material which exists in three main crystallographic phases at atmospheric pressure: (i) monoclinic (*m*, stable up to 1205 °C), (ii) tetragonal (*t*, stable from 1205 to 2377 °C) and (iii) cubic (*c*, stable from 2377 to 2710 °C) [3]. Since zirconia exhibits very low thermal conductivity (1.2- 2.6 $Wm^{-1}K^{-1}$ [4]) this makes zirconia a material of choice for thermal barrier coatings (TBCs) [5]. However, the use of zirconia is restricted by the change in its lattice volume (~5 Vol.%) [6] due to phase transformation at high temperatures. This phase transformation and change in lattice volume leads to the formation of cracks in the coating and thus failure of the device. In the last couple of decades, phase transformation of zirconia at high temperatures is avoided by stabilizing the high temperature *c*-phase of zirconia at room temperature. Typically, stabilization is achieved by doping zirconia with cations of lower valence than Zr e.g., Y or Ca. It is found that doping by 12 mol.% of yttria (Y_2O_3) leads to the stabilization of *c*-phase of zirconia at room temperature and is known as Yttria Stabilized Zirconia (YSZ) [7]. Recently, Raza *et al.* [8] unambiguously demonstrated that the stabilization of the *c*-phase of zirconia at room temperature solely dependent on the $V_{\ddot{O}}$ concentration as low as 3 at.% in the zirconia lattice. Such oxygen vacancy stabilized zirconia (OVSZ) thin films could be a great alternate of YSZ thin films for TBCs, oxygen sensors and particularly for SOFCs provided their reliable thermal stability.

In the present work, we report the thermal stability i.e., chemical and crystal structure stability of OVSZ thin films synthesized by dc-reactive magnetron sputtering. Temperature-resolved Grazing Incidence X-ray Diffraction (TR-GIXRD) measurements are performed in air and nitrogen ambient.

Experimental

Two set of OVSZ (c-ZrO_{2-x}) thin films containing ~16 (x=0.31) and 3 (x=0.06) at.% $V_{\ddot{O}}$ of thickness 100±10 nm were deposited by working inside the so-called transition zone using direct current Reactive Magnetron Sputtering (dc-RMS), as shown in Fig. 1. Films were deposited on Si(100) substrates whose thickness is 525 ±20 µm (Siegert Wafer) as well as on graphite sheet for chemical composition analysis. Those samples were deposited from a zirconium target (purity 99.97%, 5 cm in diameter) bought from Kurt J. Lesker, sputtered in argon-oxygen plasma. To work inside the transition zone, a voltage feedback control unit Speedflo mini from Gencoa, was implemented in order to provide a rapid control over O_2 partial pressure and deposit oxygen deficient zirconia films. During the deposition, substrates were placed at 6.5 cm from the Zr target. To sputter the Zr target, cathode was fed with 200 mA of discharge current by an Advanced Energy MDX 500 DC power supply equipped with an arc suppressor (Sparkle from Advanced Energy). During the deposition, O_2 was injected at the target surface and Ar was injected away from the target surface. Total working pressure was kept constant at 1.33 Pa. During the deposition no intentional heating or bias was applied to the substrate. Prior to the deposition, the substrates were cleaned with methanol in an ultrasonic bathtub for 10 minutes. To minimize possible impurities in the deposited films, each time a base pressure $< 4\times10^{-4}$ Pa was reached inside the vacuum chamber. Oxygen vacancy concentration in the as deposited films was measured from a combination of Rutherford Back Scattering (RBS) and Nuclear Reaction Analysis (NRA), as reported in [17]. The latter method was used to detect isotopic oxygen (^{18}O) which was specifically admixed to the argon gas

during some deposition runs. This way, one could distinguish the oxygen atoms incorporated in the film during the deposition process from the one incorporated in the film upon venting the samples. The crystallographic information of the as-deposited oxygen-deficient films was obtained first by Grazing Incidence X-Ray Diffraction (GIXRD) which was performed using PANalytical Empyrean with a radiation source λ = 0.15418 nm (value averaged over the Cu $K_{\alpha1}$ and $K_{\alpha2}$ lines). The diffractograms were recorded with a step size of 0.07° and a duration of 15 seconds using an incidence angle of 0.5° at 40 mA, 45 kV of generator settings. Detailed study regarding deposition, chemical composition analysis, characterization of *c*-phase and *c*-phase stabilization of OVSZ thin films can be found in Raza *et al.* [8,9] work.

Temperature resolved XRD measurements were performed on a Bruker D8 Discover diffractometer, using a Co-K_{α} radiation (λ = 0.17902 nm) and a parallel beam with a diameter of 1 mm. Samples were annealed with a heating speed of 8 °C/s either in air or in N_2 ambient, with a Domed Hot Stage (DHS1100) from Anton Paar installed on the goniometer. During annealing in the N_2 ambient, a flow of 1-2 l/h of N_2 was blown at the sample surface and the pressure inside the dome was same as outside the dome, i.e. 1 atm. This way sample surface was prevented to interact with air from surrounding during annealing. The measurements were carried out in grazing incidence geometry at a grazing angle of 3° with a step size of 0.025°, and duration of 4 s. During the scan, for each working temperature, the annealing stage temperature was kept constant for 2 hours to allow the scan to complete at that specific temperature. Further, the detection was assured by a scintillator counter in front of which long Sollers slits were installed to select the diffracted X-rays.

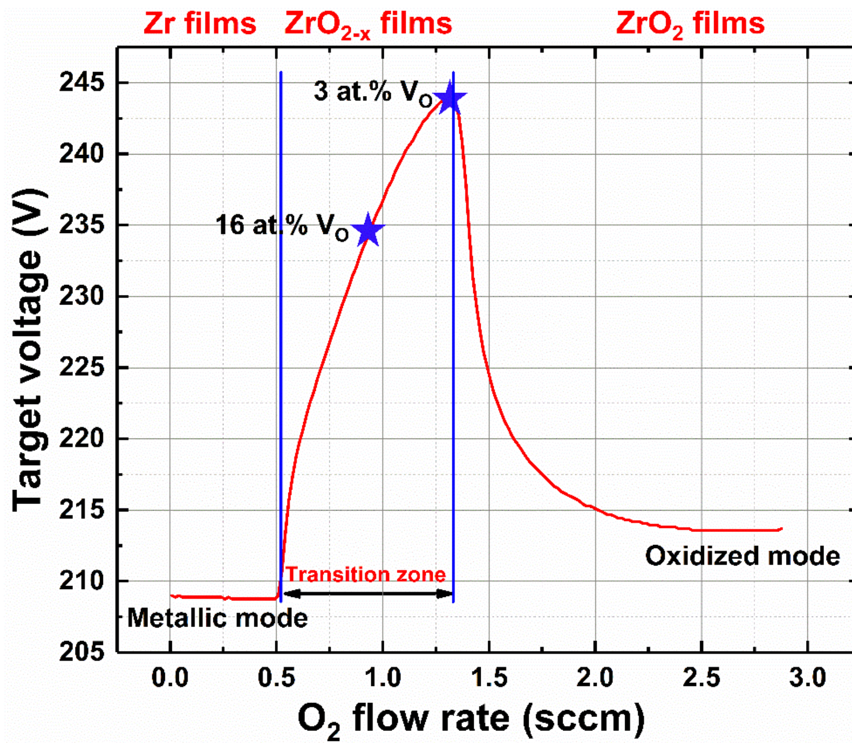

Figure 1: Target voltage curve of Zr as a function of O_2 flow rate, colour filled stars points the position where the films containing 16 and 3 at.% O vacancies were obtained.

Results and Discussion

GIXRD patterns of the as-deposited films containing 16 and 3 at.% $V_{\ddot{O}}$ acquired at an incidence angle of 0.5° are shown in Fig. 2. The diffraction peaks are identified from the zirconia *c*-phase (ICDD PDF# 49-1642).

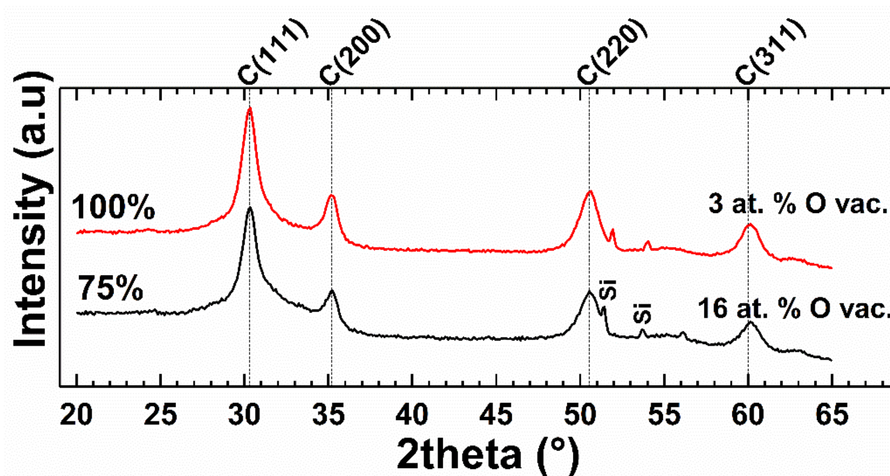

Figure 2: GIXRD patterns of the as-deposited films recorded using Cu x-ray source at an incidence angle of 0.5° at room temperature.

TR-GIXRD patterns acquired at an incidence angle of 3° for the same films containing 16 and 3 at.% $V_{\ddot{O}}$ and annealed in air and N_2 from 200 °C to 900 °C are shown in Fig. 3. It is observed in Fig. 3, the diffraction peaks are less intense than in the case of Fig. 2. Such reduced intensity of the GIXRD patterns collected as a function of temperature is primarily due to the dome utilized for the control of atmosphere and temperature, which attenuates the incident and diffracted beams. Moreover, in GIXRD measurements, the intensity of the diffraction peaks also depend on the incidence angle of the x-ray beam. At low incidence angles, such as in Fig. 2 where an incidence angle of 0.5° is used, the penetration depth of the beam is ~470 nm. While for the incidence angle 3° used for the measurement carried out in the case of Fig. 3, the penetration depth of the x-ray beam is ~1830 nm. This increased incidence angle makes the x-ray beam less sensitive to the 100 nm zirconia film and thus resulting in lower intensities of the diffraction peaks.

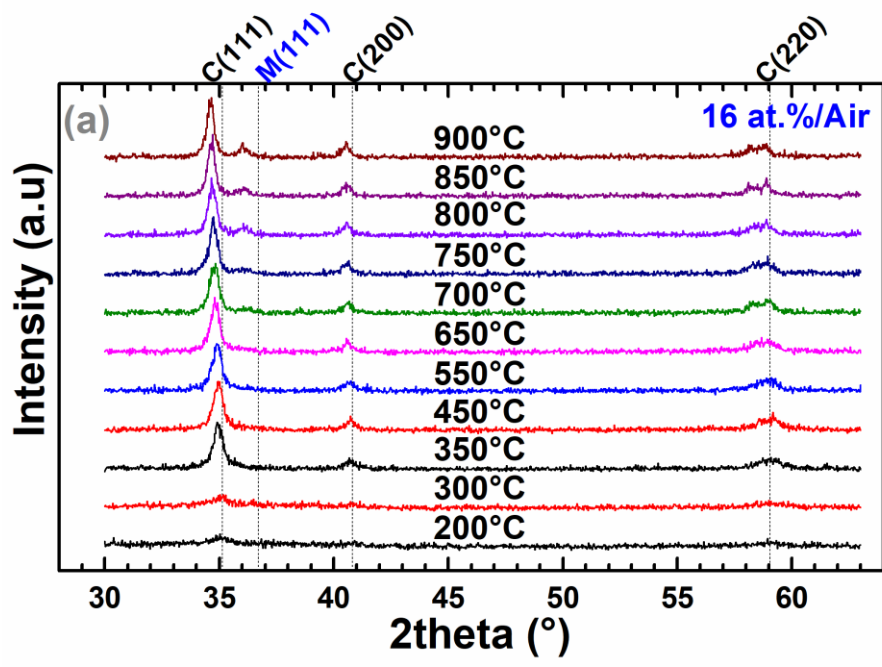
C(111)
M(111)
C(200)
C(220)
(a)
16 at.%/Air
900°C
850°C
800°C
750°C
700°C
650°C
550°C
450°C
350°C
300°C
200°C
Intensity (a.u)
30
35
40
45
50
55
60
2theta (°)

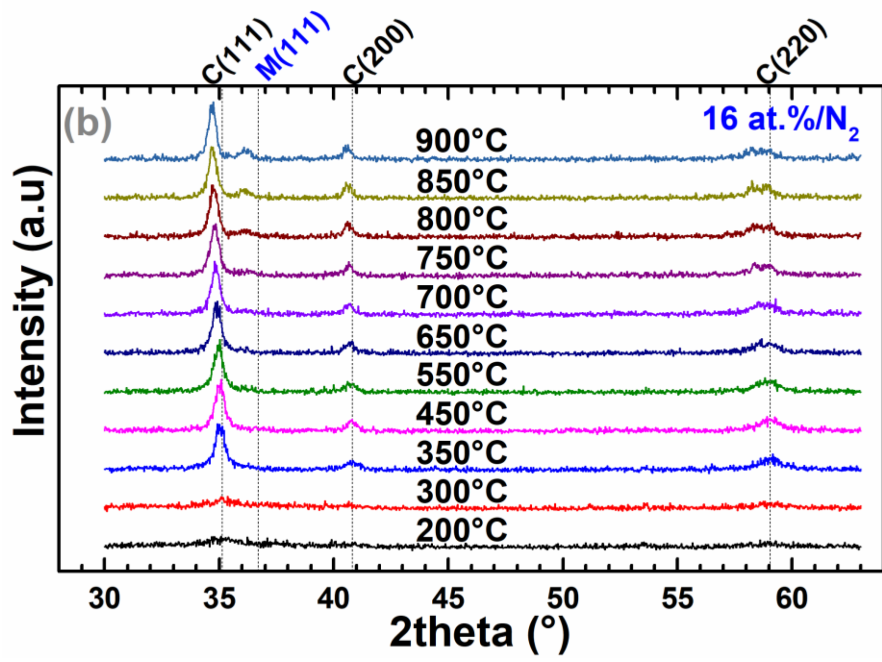
C(111)
M(111)
C(200)
C(220)
(b)
16 at.%/N2
900°C
850°C
800°C
750°C
700°C
650°C
550°C
450°C
350°C
300°C
200°C
Intensity (a.u)
30
35
40
45
50
55
60
2theta (°)

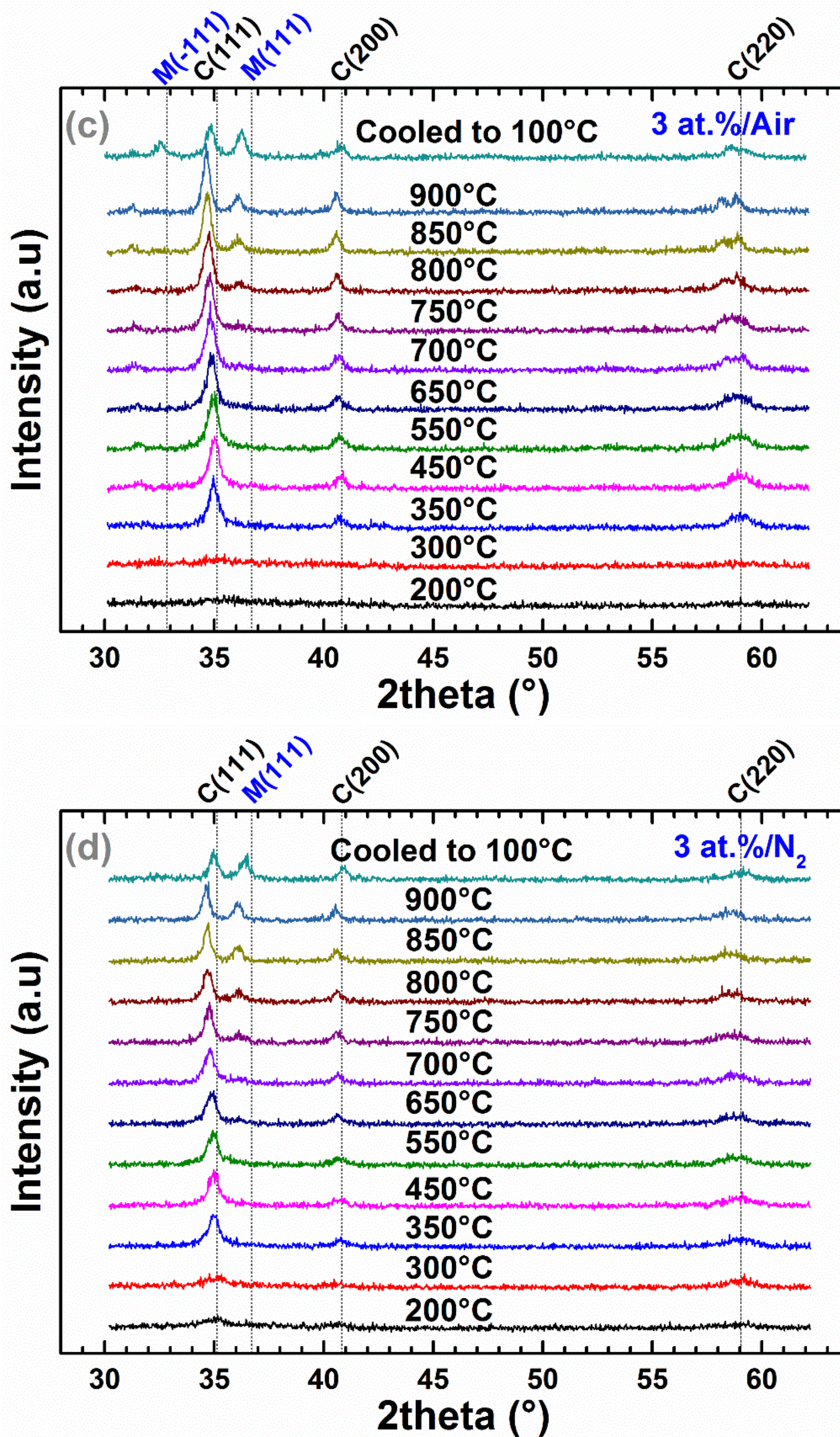

Figure 3: TR-GIXRD patterns of the films containing approximately 16 at.% O vacancies annealed in **(a)** air and **(b)** N_2. Films containing 3 at.% O vacancies are also annealed in **(c)** air and **(d)** N_2. X-ray source Co and x-ray incidence angle 3° was used.

In Fig. 3 at low temperatures, i.e. from 200-300 °C, diffraction peak intensities are weak. On further annealing of films to 350 °C, diffraction patterns starts showing the diffraction peaks

coming from cubic zirconia crystals, which become more prominent with the increase in temperature. Such appearance of diffractions peaks with the increase in temperature is an indication of films getting well crystalized with the annealing. Similar behaviour of pure ZrO_2 films deposited by sol-gel method has been observed by Mehner *et.al.* [10], in their case ZrO_2 films do not show any diffraction peaks until a temperature of 475 °C is, then peaks related to tetragonal/cubic crystals appear. Further annealing of the OVSZ samples to 750 °C result in the appearance of *m*(111) diffraction peak which gets more and more prominent with the increase in temperature. It is also observed that neither the annealing ambient (i.e. air or N_2), nor the oxygen vacancy concentration has any influence on the appearance of *m*-peak. Further, on cooling of films to 100 °C, films retain both *m*- and *c*- peaks (see Fig. 3c and 3d).

As discussed above, films get well crystalized with the increase in annealing temperature. In Fig. 4, The evolution of the crystallite size as a function of temperature is shown. For both the 16 and 3 at.% $V_{\ddot{O}}$ films, crystallite size increases monotonously with the increase in temperature up to 700 °C. After passing 700 °C, a relatively steep increase is observed. Further, on cooling down the films after reaching 900 °C, it is observed in both cases that the average crystallite size remains almost the same i.e. about 20 nm. The crystallite size was calculated using the Scherrer equation [11] taking the *c*(111) peak into consideration. The instrumental broadening was not considered and neither the lattice micro-strains while calculating the

crystallite size. It should be noted that the crystallite size calculated in this work are just to understand the trend and not to have the absolute values of crystallite size.

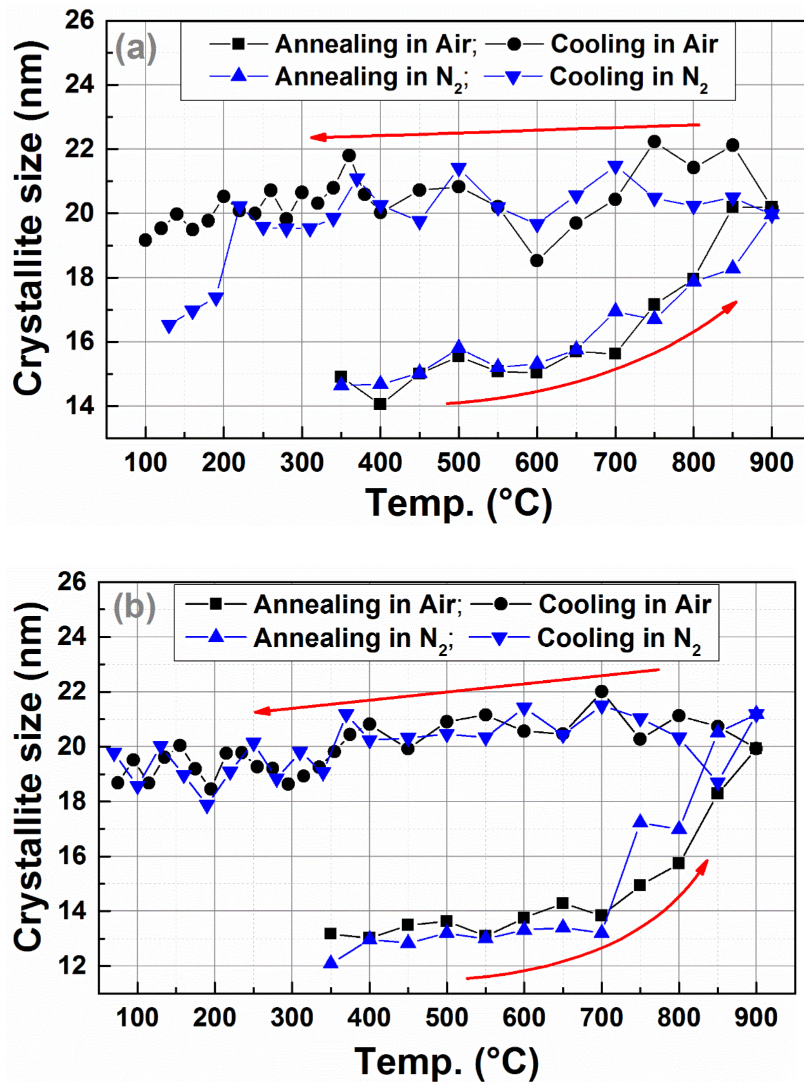

Figure 4: Evolution of cubic crystallite size as a function of temperature, calculated using *c*(111) peak of films containing (a) 16 at. % O vacancies and (b) 3 at. % O vacancies.

Further analysis of the temperature–resolved diffraction data of films containing 16 and 3 at.% $V_{\ddot{O}}$ reveal, in both cases, that the area under the *c*(111) peak increase with increasing the temperature (Fig. 5). The increase in area of *c*(111) peak is steep till 350 °C and is almost steady up to 750 °C. However, after passing 750 °C, area under the *c*(111) starts to decrease (Fig. 5). On the other hand, at this precise temperature, the *m*(111) peak appears (Fig. 3). The

variation of the area under the m(111) peak as a function of temperature is almost identical in absolute values to the decrease in area under the c(111) peak, shown in Fig. 5. Such a decrease in area under the c(111) peak after passing 750 °C indicates the transformation of cubic zirconia crystals into monoclinic zirconia crystals.

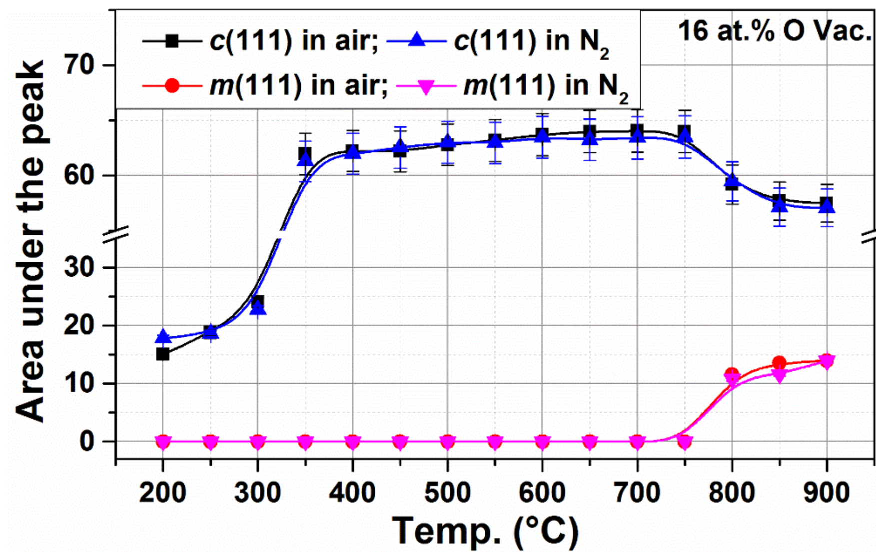

Figure 5: Area under the *c*(111) and *m*(111) peak as a function of temperature of film containing 16 at.% O vacancies. After passing the 750 °C a drop in *c*(111) and increase in *m*(111) peak area is observed. Same trend is observed for films containing 3 at.% O vacancies (data not shown here).

With the increase in annealing temperature, a shift of diffraction peaks to lower angles could be observed as well in Fig. 3, irrespective of the concentration of oxygen vacancies (16 and 3 at.%) or the annealing ambient (air or N_2). The magnitude of the peak shift is plotted in Fig.6.

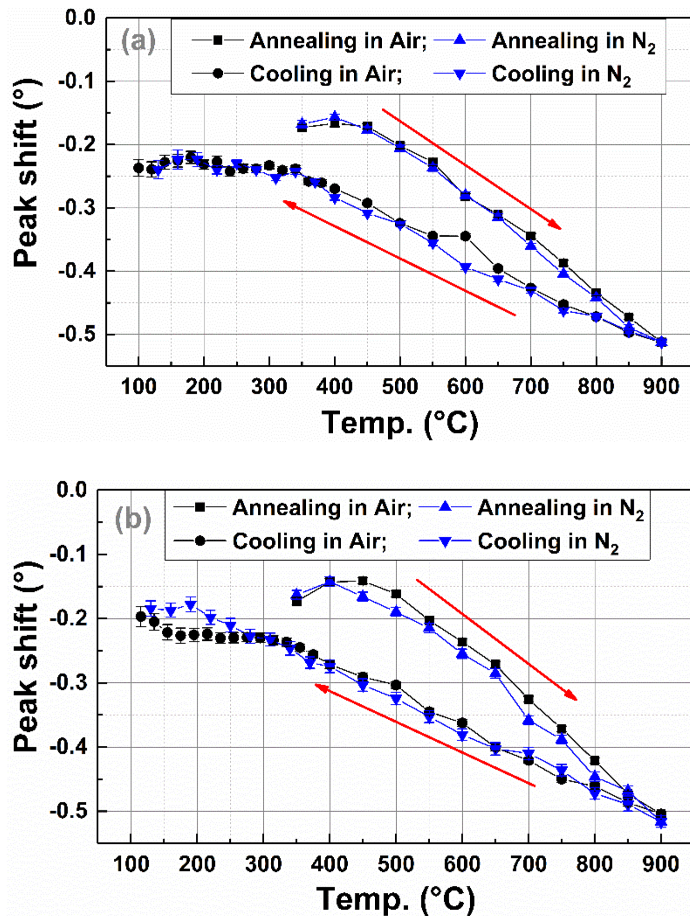

Figure 6: Shift of *c*(111) peak as a function of temperature of the films containing **(a)** 16 at.% of O vacancies **(b)** 3 at.% of O vacancies to lower angles during annealing in Air and N_2 and recovery while cooling down. Red arrows indicate whether the peak shift is measured during the annealing or cooling.

It can be seen in Fig. 6 that, at 350 °C, the *c*(111) peak exhibits a shift of less than 0.2°. With the increase in annealing temperature, the *c*(111) peak shifts further to lower angles. At 900 °C, a shift to lower angle of about 0.5° is reached as shown in Fig. 3 and Fig. 6. The *c*(311) peak appearing at 70.66° also shifts by 0.2° when T = 750 °C. This peak shift further by 0.4° when a temperature of 900 °C is reached. While on cooling down the films, it is observed that the *c*(111) peak tries to return to its original position. One should also note that the *m*(111) peak also did not vanish upon cooling. It is also observed from Fig. 3 and Fig. 6 that the films containing 16 and 3 at.% $V_{\ddot{O}}$ and annealed in air and N_2 show similar evolution. Mehner *et al.*

also observed such peak shifts on annealing their zirconia thin films to 750 °C [10]. Their study highlighted a correlation between the peak shift, the appearance of the monoclinic phase, and the evolution of stress in the film as a function of temperature. It is known that stress in as-deposited films can develop as a result of deposition conditions [12] (known as intrinsic stresses) as well as during annealing because of the difference in film-substrate thermal expansion coefficients (TECs). Since Si has a lower TEC (3.6×10^{-6}/K [13]) as compared to *c*-zirconia (8.8-10.6×10^{-6}/K [4]) and as the deposited film is bound to the substrate, therefore, at elevated temperature, the OVSZ film will experience compressive stresses. This will cause diffraction peaks to shift to the lower angles in the diffraction patterns, as seen in Fig. 3 and Fig. 6. Such thermal stresses were calculated using Eq. 1 where E_f is the Young's modulus, v_f is the Poisson ratio, α_f and α_s are the respective TECs of the film and substrate, T_s is the substrate temperature during deposition (25 °C), and T_a is the temperature during the measurement [14]. A negative value of σ_{th} corresponds to compressive stress.

$$\sigma_{th} = \frac{E_f}{1 - v_f}\left(\alpha_f - \alpha_s\right)(T_s - T_a) \quad (1)$$

To calculate theoretical thermal stress values in deposited films, the Young's modulus and Poisson ratio was taken from the literature (E_{f} =200 GPa [15,16], $v_f = 0.25$ [10]) and was assumed that the zirconia Young's modulus variation with the temperature is negligible. The calculated compressive stress was found to increase with the increase in temperature, Fig. 7. Calculation indicates that at 750 °C, the film stress reaches a value of -856 MPa. At 900 °C, the value reaches -1032 MPa.

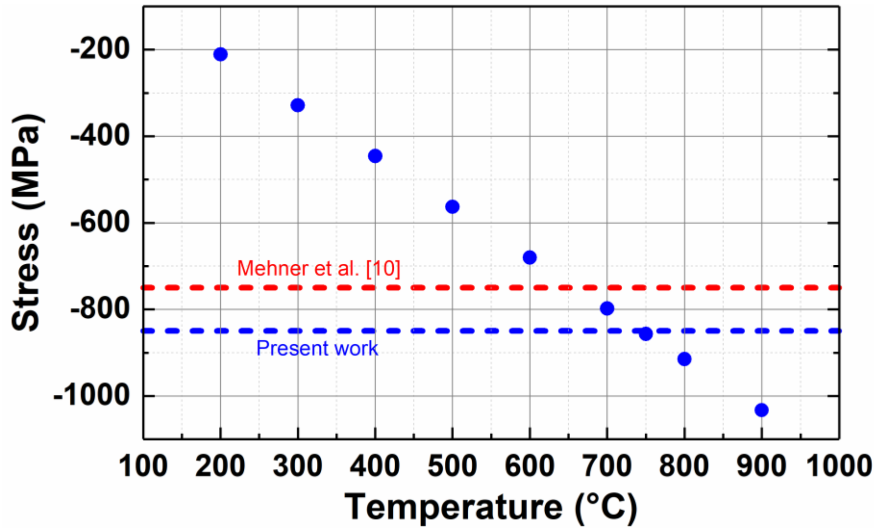

Figure 7: Evolution of compressive stresses in the films containing 16 and 3 at.% of O vacancies annealed in air and N_2 ambient. Stress is assumed to be induced by the discrepancy of TEC between the OVSZ film and the Si substrate. The critical stress at which zirconia cubic film turns to mixed cubic and monoclinic phase. Stress value reported in the work of Mehner et al [10] is presented for comparison.

From the above presented data, appearance of monoclinic crystals after passing 750 °C at first could be related to annihilation of $V_{\ddot{O}}$ present in the OVSZ films by uptake of oxygen from the surrounding ambient since OVSZ films, by definition are under-stoichiometric films, and oxygen vacancies are the sole responsible mechanism for stabilizing zirconia cubic structure [8]. Monoclinic crystal structure is thermodynamically the most stable for fully stoichiometric zirconia (ZrO_2) below ~ 1200 °C. But it can be also observed in Fig. 3 that diffraction peak related to *c*-phase remain at 900 °C and even when cooled down to 100 °C. Since $V_{\ddot{O}}$ promotes the formation of *c*-phase at low temperatures as Raza *et al.* [8] has shown, therefore, it would be inappropriate to say that the O vacancies are annihilated and film turned stoichiometric (ZrO_2). Furthermore, the diffractograms of all the OVSZ films have a similar evolution with the annealing temperature, whatever they contain 3 or 16 at.% oxygen vacancies or they annealed in air or nitrogen atmosphere. This situation highlights that the presence of oxygen in the annealing ambient does not affect the phase transformation. On the other hand, the transformation of cubic crystals into monoclinic crystals could be related to the martensitic transformation caused by compressive stresses after passing a critical temperature where the

compressive stresses are building up inside the film during annealing due to the difference in film-substrate TECs. in the present case, it can be assumed that the appearance of *m*-peaks on the diffractogram, as shown in Fig. 3, is the achievement of critical stress at 750 °C. Similar phenomenon i.e., the appearance of *m*-phase as a result of compressive stresses in zirconia films of thickness 100-150 nm, was reported by Ngaruiya *et al.*[17] and Goedicke *et al.*[12]. Ngaruiya *et al.*[17] have shown how the film stress evolves as a function of oxygen flow rate during reactive magnetron sputtering experiments. According to Ngaruiya *et al.* [17], when the oxygen flow rate is low i.e. the sputter target is not fully oxidized and the films exhibit low compressive stress values. As the target gets fully oxidized when higher oxygen flow rates are used, films exhibit high compressive stress close to -1500 MPa and zirconia films are observed to form monoclinic crystals. Goedicke *et al.*[12] also studied the generation of stress in zirconia coatings as a function of sputtering pressure, using pulsed magnetron sputtering. From their study, it seems that working at high pressures i.e. 3.5 Pa, lead to tensile stress of approximately 150 MPa in the films. In this case the films XRD patterns exhibited only cubic reflections. However, when the films were deposited at low pressure i.e. 0.3 Pa, films exhibited high compressive stress (-1800 MPa) and only monoclinic reflections were observed. It is similar to *c/t* – to – *m* phase transformation in sol-gel based ZrO_2 films [10] or stress/pressure induced *t* – to – *m* phase transformation in YSZ [18–20]. Mehner *et al.* [10] deposited *c/t* 1000 – 1200 nm thick zirconia films on steel substrates using sol-gel method and studied their thermal stability. Their cubic/tetragonal zirconia films were stable up-to 600 °C and above this temperature monoclinic peaks appeared on their XRD patterns. They also observed a small shift in the peak position to lower angles with the increase in temperature, like the shift monitored in the present study. Mehner *et al.* [10] attributed the shift to the generation of compressive stresses in the film during annealing. *t*-phase transformation into monoclinic has also been studied by Allahkarami *et al.*[19,20] who applied a local compressive load on *t*-YSZ.

After applying the load, t – to – m phase conversion up to 100% was observed in that area. Moreover, t – to – m phase transformation in YSZ films has been reported by Piascik *et al.*[18] who varied the bias applied to the substrate holder during deposition. Doing so, ion bombardment during film growth is intensified as the bias voltage/power is increased. The bias power was applied to vary film stresses. These authors claim that the t – to - m phase transformation occurs when the film stress reaches a critical threshold level, although no values were reported in their paper. According to the reported literature and the data presented in the current study, it seems reasonable to assume that OVSZ thin films reached a critical compressive stress value after passing 750 °C, and such compressive stress forced cubic crystals to transform into monoclinic ones. Finally, thermal cycling (6 times) of the OVSZ thin films to 700 °C showed no sign of appearance of *m*-phase i.e., films preserved their pure *c*-phase.

Conclusion

Thermal stability of oxygen vacancy stabilized zirconia (OVSZ) thin films containing 16 and 3 at.% oxygen vacancies, deposited by dc-reactive magnetron sputtering on Si(100) substrate is reported in this paper. From our data, it is observed that OVSZ thin films deposited on Si(100) substrates are stable up-to 750 °C irrespective of annealing ambient i.e., air or N_2. However, above 750 °C, the temperature resolved grazing incidence x-ray diffraction patterns showed diffraction peak related to the presence of monoclinic crystals, which did not disappear on cooling down the films. the transformation of a fraction of cubic crystals into monoclinic crystals above 750 °C most likely originated from increased compressive stress above a threshold value i.e., -850 MPa in our conditions, caused by the difference in thermal expansion coefficient of OVSZ thin film and the Si substrate. However, OVSZ thin subjected to thermal

cycling up to 700 °C showed no sign of appearance of *m*-phase i.e., films preserved their pure *c*-phase. These findings suggest OVSZ thin films could be a promising alternate of yttria stabilized zirconia (YSZ) in devices needing operating temperature around or below 750 °C, as reported in M. Raza *et al*. [21].

Acknowledgement

This work is supported by the Belgian Government through the «Pôle d'Attraction Inter universitaire» (PAI, "Plasma-Surface Interaction", Ψ). S. Konstantinidis is a Senior Research Associate of the FNRS (Fonds National de la Recherche Scientifique), Belgium.

References

[1] R. Arróyave, D.L. McDowell, Systems Approaches to Materials Design: Past, Present, and Future, Annu. Rev. Mater. Res. 49 (2019) 103–126. https://doi.org/10.1146/annurev-matsci-070218-125955.

[2] G.B. Olson, Computational Design of Hierarchically Structured Materials, Science (80-.). 277 (1997) 1237–1242. https://doi.org/10.1126/science.277.5330.1237.

[3] J.P. Abriata, J. Garcés, R. Versaci, The O-Zr (Oxygen-Zirconium) system, Bull. Alloy Phase Diagrams. 7 (1986) 116–124. https://doi.org/10.1007/BF02881546.

[4] D. Stöver, G. Pracht, H. Lehmann, M. Dietrich, J.-E. Döring, R. Vaßen, New Material Concepts for the Next Generation of Plasma-Sprayed Thermal Barrier Coatings, J. Therm. Spray Technol. 13 (2004) 76–83. https://doi.org/10.1361/10599630418176.

[5] D.R. Clarke, S.R. Phillpot, Thermal barrier coating materials, Mater. Today. 8 (2005) 22–29. https://doi.org/10.1016/S1369-7021(05)70934-2.

[6] S. Shukla, S. Seal, Mechanisms of room temperature metastable tetragonal phase stabilisation in zirconia, Int. Mater. Rev. 50 (2005) 45–64. https://doi.org/10.1179/174328005X14267.

[7] J.R. Kelly, I. Denry, Stabilized zirconia as a structural ceramic: an overview., Dent. Mater. 24 (2008) 289–98. https://doi.org/10.1016/j.dental.2007.05.005.

[8] M. Raza, D. Cornil, J. Cornil, S. Lucas, R. Snyders, S. Konstantinidis, Oxygen Vacancy Stabilized Zirconia (OVSZ); A Joint Experimental and Theoretical Study, Scr. Mater. 124 (2016) 26–29. https://doi.org/10.1016/j.scriptamat.2016.06.025.

[9] M. Raza, S. Sanna, L. dos Santos_Gómez, E. Gautron, A.-A. El Mel, N. Pryds, R. Snyders, S. Konstantinidis, V. Esposito, Electronic supplementary information (ESI) for Near interface ionic transport in oxygen vacancy stabilized cubic zirconium oxide thin films, Phys. Chem. Chem. Phys. (2018). https://doi.org/10.1039/C8CP05465G.

[10] A. Mehner, H. Klümper-Westkamp, F. Hoffmann, P. Mayr, Crystallization and residual stress

formation of sol-gel-derived zirconia films, Thin Solid Films. 308–309 (1997) 363–368. https://doi.org/10.1016/S0040-6090(97)00579-8.

[11] A.L. Patterson, The scherrer formula for X-ray particle size determination, Phys. Rev. 56 (1939) 978–982. https://doi.org/10.1103/PhysRev.56.978.

[12] K. Goedicke, J. Liebig, O. Zywitzki, H. Sahm, Influence of process parameters on the structure and the properties of ZrO 2 coatings deposited by reactive pulsed magnetron sputtering (PMS), Thin Solid Films. 377–378 (2000) 37–42.

[13] W.M. Yim, R.J. Paff, Thermal expansion of AlN, sapphire, and silicon, J. Appl. Phys. 45 (1974) 1456–1457. https://doi.org/10.1063/1.1663432.

[14] Y. Pauleau, Generation and evolution of residual stresses in physical vapour-deposited thin films, Vacuum. 61 (2001) 175–181. https://doi.org/10.1016/S0042-207X(00)00475-9.

[15] R. Morrell, Handbook of Properties of Technical and Engineering Ceramics, Her Majesty's Stationary Office, London, 1985.

[16] E.H. Kisi, C.J. Howard, Crystal Structures of Zirconia Phases and their Inter-Relation, Key Eng. Mater. 153–154 (1998) 1–36. https://doi.org/10.4028/www.scientific.net/KEM.153-154.1.

[17] J.M. Ngaruiya, O. Kappertz, S.H. Mohamed, M. Wuttig, Structure formation upon reactive direct current magnetron sputtering of transition metal oxide films, Appl. Phys. Lett. 85 (2004) 748. https://doi.org/10.1063/1.1777412.

[18] J.R. Piascik, Q. Zhang, C.A. Bower, J.Y. Thompson, B.R. Stoner, Evidence of stress-induced tetragonal-to-monoclinic phase transformation during sputter deposition of yttria-stabilized zirconia, J. Mater. Res. 22 (2007) 1105–1111. https://doi.org/Doi 10.1557/Jmr.2007.0128.

[19] M. Allahkarami, J.C. Hanan, Residual Stress and Phase Transformation in Zirconia Restoration Ceramics, Adv. Bioceram. Porous Ceram. V Ceram. Eng. Sci. Proc. 574 (2012) 37. https://doi.org/10.1002/9781118217504.ch6.

[20] M. Allahkarami, J.C. Hanan, Mapping the tetragonal to monoclinic phase transformation in zirconia core dental crowns, Dent. Mater. 27 (2011) 1279–1284. https://doi.org/10.1016/j.dental.2011.09.004.

[21] M. Raza, S. Sanna, L. Dos Santos Gómez, E. Gautron, A.A. El Mel, N. Pryds, R. Snyders, S. Konstantinidis, V. Esposito, Near interface ionic transport in oxygen vacancy stabilized cubic zirconium oxide thin films, Phys. Chem. Chem. Phys. 20 (2018) 26068–26071. https://doi.org/10.1039/c8cp05465g.